Extinction in host-vector infection models and the role of heterogeneity

Mathematical Biosciences 367 (2024) 109108

Contents lists available at ScienceDirect

Mathematical Biosciences

journal homepage: www.elsevier.com/locate/mbs

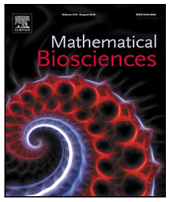

Original Research Article

Extinction in host–vector infection models and the role of heterogeneity

Damian Clancy *, John J.H. Stewart

Department of Actuarial Mathematics and Statistics, Maxwell Institute for Mathematical Sciences, Heriot-Watt University, Edinburgh, EH14 4AS, UK

ARTICLE INFO

MSC:
92D30
60J27

Keywords:
Persistence time
Endemic fade-out
Stochastic epidemic models
Multi-patch models

ABSTRACT

For infections that become endemic in a population, the process may appear stable over a long time scale, but stochastic fluctuations can lead to eventual disease extinction. We consider the effects of model parameters and of population heterogeneities upon the expected time to extinction for host–vector disease systems. We find that non-homogeneous host selection by vectors increases persistence times relative to the homogeneous case, and that the effect becomes even more marked when there are strong associations between particular groups of vectors and hosts. Heterogeneity in vector lifespans, in contrast, is found to decrease persistence times relative to the homogeneous case. Neither the basic reproduction number R_0, nor the endemic prevalence level in the corresponding deterministic model, is found to be sufficient to predict (for a given population size) time to extinction. The endemic level, in particular, proves a very unreliable guide to the duration of long-term persistence.

1. Introduction

Many infections that impact significantly upon human and animal health are vector borne. The classic example from a mathematical modelling perspective is malaria, which is transmitted via mosquitoes, and was first modelled by Ross [1]. Other important vector borne infections include dengue fever, yellow fever, and Zika virus disease. The deterministic modelling framework of [1] was later extended by Macdonald [2], and deterministic models have continued to be widely used in modelling vector borne infections. However, in some contexts stochastic effects cannot be ignored. For instance, immediately following the introduction of infection into a population, stochastic effects determine whether the infection rapidly dies out or spreads through the population. If an infection becomes endemic, then stochasticity produces variations in prevalence around the endemic level. Finally, stochastic effects can lead to eventual disease extinction. A stochastic counterpart of the Ross–Macdonald model, which we describe in Section 2, has been developed and analysed by a number of authors [3–5].

The simplest mathematical models assume homogeneity of the host and vector populations. In reality, a variety of forms of heterogeneity may be present. For instance, malaria can be transmitted to humans by a number of different species of *Anopheles* mosquito, and estimates of mean lifespan differ between species [6]. There is evidence that mosquitoes tend to bite some people more frequently than others, with the biting rate on a particular individual potentially depending on factors such as their age, size, blood group, or proximity to a mosquito breeding site [7]. Thus both host and vector populations may be divided into a number of types, which may represent geographical 'patches', or other characteristics such as species (of vector) or age groups (of host). Such heterogeneities can be important to take into account in the design of control strategies.

In [7,8], a deterministic model was developed that extends the Ross–Macdonald model to allow for non-homogeneous mixing between vectors and hosts. The effects were studied of such heterogeneity upon the host-to-host basic reproduction number R_0 (the average number of secondary host infections that arise from a single infected host introduced into an otherwise susceptible population), and upon the endemic prevalence level. A stochastic version of the model of [7,8] was developed in [4], and used to study the probability of successful disease invasion, as well as to quantify, in the case that the disease does successfully invade, the variability in prevalence about the mean endemic level. Thus [4,7,8] consider the early (invasion into a naive population) and secondary (endemic) phases of a disease outbreak. Our focus in the current work will be on the late phase; that is, we study the time from endemicity to disease extinction. For a homogeneous population model, this late phase has been previously considered in [5]. The work of [5] relies upon a bivariate normal approximation to the quasistationary distribution of the process. The quasistationary distribution (defined precisely in Section 2) describes the behaviour of the process during the endemic phase, prior to eventual extinction, when the process may exhibit apparently stable behaviour over quite a long time scale. The bivariate normal distribution provides a good

* Corresponding author.
E-mail addresses: d.clancy@hw.ac.uk (D. Clancy), js140@hw.ac.uk (J.J.H. Stewart).

https://doi.org/10.1016/j.mbs.2023.109108
Received 18 August 2023; Received in revised form 16 October 2023; Accepted 12 November 2023
Available online 7 December 2023

approximation to the central part of the quasistationary distribution, and hence provides an appropriate tool to quantify variability about the endemic prevalence level [4], but fails in the tail of the distribution close to extinction — see, for instance, Fig. 3 of [4]. Consequently, this approximation leads to very poor approximations for the mean time to extinction [9]. Indeed, it is remarked in [5] that a possibility for improvement would be to obtain a better approximation of the quasistationary distribution close to extinction. This improvement is one that we carry out in Section 2 below, developing a WKB (Wentzel, Kramers, Brillouin) approximation to the quasistationary distribution that improves upon the bivariate normal approximation in the relevant tail of the distribution. We go on in Section 3 to extend our methodology to allow for population heterogeneities.

The remainder of the paper is structured as follows. In Section 2, we describe the stochastic version of the Ross–Macdonald model, setting out some standard theory relating to the basic reproduction number R_0, the quasistationary distribution of the process and its WKB approximation. Using the WKB technique we obtain an approximation to the mean time to extinction for the process started from quasistationarity, and study the effect of varying model parameters upon extinction time. We also investigate the accuracy of our approximation. In Section 3 we set out the stochastic Ross–Macdonald model in a heterogeneous population, extending our WKB approximation to allow for such heterogeneity, and study the effect of various forms of heterogeneity upon extinction time. Finally, in Section 4, we summarise our main results and present some further discussion.

2. The stochastic Ross–Macdonald model

2.1. Model framework and methodology

Consider a population of hosts and vectors with deaths and births balanced to give a fixed population size for each. Denote by N the host population size and by V the vector population size, and define $c = V/N$ to be the number of vectors per host. We assume that each host and each vector is, at any point in time, either susceptible to infection, or infected and infectious. The lifespan of a vector is assumed short enough that an infected vector will die before it recovers. Recovered hosts are assumed to be immediately susceptible to re-infection, with no period of immunity. Denote by $Y_H(t)$ the number of infected hosts and by $Y_V(t)$ the number of infected vectors at time t. Then since population sizes are fixed, we have $N - Y_H(t)$ susceptible hosts and $V - Y_V(t)$ susceptible vectors at time t. A single vector bites hosts at rate k. When an infected vector bites a susceptible host, infection is transmitted from vector to host with probability p. When a susceptible vector bites an infected host, infection is transmitted from host to vector with probability q. Hosts do not infect other hosts and vectors do not infect other vectors. A host that becomes infected remains so for an exponentially distributed period of time with mean $1/\sigma$ before recovery. A vector that becomes infected remains so until its death, which occurs after an exponentially distributed period of time with mean $1/\delta$, and is then immediately replaced by a new susceptible vector. We assume throughout that $N, V, k, p, q, \sigma, \delta > 0$. A key feature of the model is the asymmetry between hosts and vectors — the rate at which a vector bites hosts is assumed independent of the number of hosts present, whereas the rate at which a host receives bites is proportional to the number of vectors present.

A summary of model parameters is given in Table 1 along with reference values (unit of time being years). Literature references for each of these values, as appropriate for malaria in a population of human hosts and mosquito vectors, may be found in Section 6 of [5]. In Section 2.3 we will investigate the effect of varying parameter values from these baseline values.

The host-to-host basic reproduction number R_0 is given by [4]

$$R_0 = \frac{cpqk^2}{\sigma\delta}. \tag{1}$$

Table 1
Reference parameter values (time units of years), from [5].

Parameter	Reference value	Description
c	5	Number of vectors per host
k	73	Biting rate per vector (bites per year)
p	0.5	Vector to host transmission probability
q	0.15	Host to vector transmission probability
σ	0.014^{-1}	Recovery rate of infected host
δ	0.055^{-1}	Death rate of infected vector

Table 2
Transition rates for the stochastic Ross–Macdonald model.

Event	State transition	Transition rate
Infection of a host	$(Y_H, Y_V) \to (Y_H + 1, Y_V)$	$kpY_V\left(N - Y_H\right)/N$
Infection of a vector	$(Y_H, Y_V) \to (Y_H, Y_V + 1)$	$kq(V - Y_V)Y_H/N$
Recovery of a host	$(Y_H, Y_V) \to (Y_H - 1, Y_V)$	σY_H
Death of a vector	$(Y_H, Y_V) \to (Y_H, Y_V - 1)$	δY_V

If $R_0 \leq 1$, then any outbreak of infection is guaranteed to die out quickly, whereas if $R_0 > 1$ there is a positive probability of successful invasion leading to infection becoming endemic in the population. These statements can be made precise in terms of a branching process approximation valid in the early stages of disease invasion [10]. For the parameter values of Table 1, $R_0 \approx 1.54$.

Writing $\boldsymbol{Y}(t) = (Y_H(t), Y_V(t))$, then the process $\{\boldsymbol{Y}(t) : t \geq 0\}$ is a Markov process on the finite state space $S = \{(y_H, y_V) \in \mathbb{Z}_+^2 : 0 \leq y_H \leq N,\ 0 \leq y_V \leq V\}$ with transition rates given in Table 2. The state space S consists of an absorbing state at $(0,0)$, the disease-free state, and a transient communicating class $C = S \setminus \{(0,0)\}$. It follows that, regardless of parameter values or initial state, the process will almost surely be absorbed into state $(0,0)$ within finite time; that is, the infection will eventually die out from the population.

In the large population limit, so long as numbers of individuals in each category remain large, the infection process can be approximated by a deterministic process. More precisely, consider the limit as $N \to \infty$ with $c = V/N$ held constant. The process $\boldsymbol{Y}(t) = \left(Y_H(t), Y_V(t)\right)$ is a density-dependent process in the sense of chapter 11 of [11]; that is, transition rates are of the form

$$\Pr\left(\boldsymbol{Y}(t+\delta t) = \boldsymbol{y} + \boldsymbol{l} \mid \boldsymbol{Y}(t) = \boldsymbol{y}\right) = NW_{\boldsymbol{l}}\left(\frac{\boldsymbol{y}}{N}\right) + o(\delta t) \text{ for } \boldsymbol{y} \in S,\ \boldsymbol{l} \in L, \tag{2}$$

for some functions $W_{\boldsymbol{l}} : \mathbb{R}_+^2 \to \mathbb{R}_+$, where L is the set of possible jumps from each state $\boldsymbol{y} \in S$. From Theorem 11.2.1 of [11], the scaled process $\boldsymbol{Y}(t)/N$ converges almost surely over finite time intervals, as $N \to \infty$, to the solution $\boldsymbol{x}(t) = \left(x_H(t), x_V(t)\right)$ of the ordinary differential equation system $d\boldsymbol{x}/dt = \sum_{\boldsymbol{l} \in L} \boldsymbol{l} W_{\boldsymbol{l}}(\boldsymbol{x})$, which for our model corresponds to the system

$$\left.\begin{aligned} \frac{dx_H}{dt} &= kpx_V(1 - x_H) - \sigma x_H, \\ \frac{dx_V}{dt} &= kq(c - x_V)x_H - \delta x_V. \end{aligned}\right\} \tag{3}$$

System (3), the deterministic Ross–Macdonald model, has an equilibrium point at $(x_H, x_V) = (0,0)$, the disease free state. For $R_0 \leq 1$, this is the only feasible equilibrium, and is stable. For $R_0 > 1$, the disease free state is unstable, there is one other feasible equilibrium, the endemic equilibrium point $\boldsymbol{x}^* = (x_H^*, x_V^*)$ with components given by

$$x_H^* = \left(\frac{kpc}{kpc + \sigma}\right)\frac{R_0 - 1}{R_0}, \quad x_V^* = \left(\frac{kqc}{kq + \delta}\right)\frac{R_0 - 1}{R_0}, \tag{4}$$

and the point $\boldsymbol{x}^*$ is stable [4].

Denote by Q the transition rate matrix of the Markov process $\{\boldsymbol{Y}(t) : t \geq 0\}$, with entries given in Table 2, and by Q_C the transition rate matrix restricted to C. Then it is known [12] that there exists a unique quasistationary distribution $\boldsymbol{q} = \{q_{\boldsymbol{y}} : \boldsymbol{y} \in C\}$ such that, for any initial state within C,

$$q_{\boldsymbol{y}} = \lim_{t \to \infty} \Pr\left(\boldsymbol{Y} = \boldsymbol{y} \mid \boldsymbol{Y} \in C\right) \text{ for all } \boldsymbol{y} \in C.$$

The distribution $\boldsymbol{q}$ may be found as the unique solution of

$$\boldsymbol{q}Q_C = -(1/\tau)\boldsymbol{q} \qquad \text{with} \sum_{\boldsymbol{y}\in C} q_{\boldsymbol{y}} = 1, \tag{5}$$

where $-(1/\tau)$ is the eigenvalue of Q_C with largest real part.

For $R_0 > 1$, following a successful invasion of infection the process settles to the quasistationary distribution $\boldsymbol{q}$, before stochastic fluctuations lead to eventual disease extinction, the time to extinction from quasistationarity being exponentially distributed with mean τ. For $R_0 \leq 1$, the quasistationary distribution $\boldsymbol{q}$ still exists, but is of little practical relevance, since infection dies out quickly.

The mean time to extinction from quasistationarity, τ, may in principle be found by solving the eigenvector equation (5), but this becomes impractical for large population sizes, so instead we approximate as follows. First note that for any process with transition rates of the form (2), Eq. (5) may be written as

$$\sum_{\boldsymbol{l}\in L}\left(q_{\boldsymbol{y}-\boldsymbol{l}}W_{\boldsymbol{l}}\left(\frac{\boldsymbol{y}-\boldsymbol{l}}{N}\right) - q_{\boldsymbol{y}}W_{\boldsymbol{l}}\left(\frac{\boldsymbol{y}}{N}\right)\right) = -(\tau N)^{-1}q_{\boldsymbol{y}} \text{ for } \boldsymbol{y}\in C, \tag{6}$$

with

$$\tau = \left(N\sum_{\boldsymbol{l}\in L} q_{-\boldsymbol{l}}W_{\boldsymbol{l}}\left(-\frac{\boldsymbol{l}}{N}\right)\right)^{-1}. \tag{7}$$

Following the methodology described in [13] and references therein, we adopt the WKB *ansatz* that

$$q_{\boldsymbol{y}} = \exp\left(-NU(\boldsymbol{y}/N) + o(N)\right) \tag{8}$$

for some function $U(\boldsymbol{x})$ that does not depend upon N, with $U(\boldsymbol{x}^*) = 0$. Substituting into Eq. (6), assuming that τ is sufficiently large for the right hand side to be neglected, and collecting leading order terms, we find that $U(\boldsymbol{x})$ satisfies the Hamilton–Jacobi equation $H\left(\boldsymbol{x}, \frac{\partial U}{\partial \boldsymbol{x}}\right) = 0$ with Hamiltonian $H(\boldsymbol{x},\boldsymbol{\theta})$ given by

$$H(\boldsymbol{x},\boldsymbol{\theta}) = \sum_{\boldsymbol{l}\in L} W_{\boldsymbol{l}}(\boldsymbol{x})\left(\mathrm{e}^{\boldsymbol{l}^T\boldsymbol{\theta}} - 1\right)$$

where $\boldsymbol{\theta} = (\theta_H, \theta_V)$. Furthermore, it follows [13] from Eqs. (7) and (8) that

$$\lim_{N\to\infty}\frac{\ln\tau}{N} = U(\boldsymbol{0}). \tag{9}$$

In general, the Hamilton–Jacobi equation must be solved numerically using the method of characteristics ([14], Section 3.2). That is, we solve the characteristic ordinary differential equations (Hamilton's equations of motion) given by

$$\frac{d\boldsymbol{x}}{dt} = \frac{\partial H}{\partial \boldsymbol{\theta}}, \quad \frac{d\boldsymbol{\theta}}{dt} = -\frac{\partial H}{\partial \boldsymbol{x}}. \tag{10}$$

For the stochastic Ross–Macdonald model, the Hamiltonian is

$$\begin{aligned} H(\boldsymbol{x},\boldsymbol{\theta}) = {} & kpx_V(1-x_H)\left(\mathrm{e}^{\theta_H}-1\right) + kq(c-x_V)x_H\left(\mathrm{e}^{\theta_V}-1\right) \\ & + \sigma x_H\left(\mathrm{e}^{-\theta_H}-1\right) + \delta x_V\left(\mathrm{e}^{-\theta_V}-1\right) \end{aligned}$$

and Eqs. (10) may be written out in full as

$$\left.\begin{aligned} \frac{dx_H}{dt} &= kpx_V(1-x_H)\mathrm{e}^{\theta_H} - \sigma x_H\mathrm{e}^{-\theta_H}, \\ \frac{dx_V}{dt} &= kq(c-x_V)x_H\mathrm{e}^{\theta_V} - \delta x_V\mathrm{e}^{-\theta_V}, \\ \frac{d\theta_H}{dt} &= kpx_V\left(\mathrm{e}^{\theta_H}-1\right) - kq(c-x_V)\left(\mathrm{e}^{\theta_V}-1\right) - \sigma\left(\mathrm{e}^{-\theta_H}-1\right), \\ \frac{d\theta_V}{dt} &= kqx_H\left(\mathrm{e}^{\theta_V}-1\right) - kp(1-x_H)\left(\mathrm{e}^{\theta_H}-1\right) - \delta\left(\mathrm{e}^{-\theta_V}-1\right). \end{aligned}\right\} \tag{11}$$

Setting $\boldsymbol{\theta} = \boldsymbol{0}$ in Eqs. (11) we recover Eqs. (3), with equilibrium points at $(\boldsymbol{x},\boldsymbol{\theta}) = (\boldsymbol{0},\boldsymbol{0})$ and $(\boldsymbol{x},\boldsymbol{\theta}) = (\boldsymbol{x}^*,\boldsymbol{0})$, where the components of $\boldsymbol{x}^*$ are given by Eqs. (4). Setting $\boldsymbol{x} = \boldsymbol{0}$ in Eqs. (11) we find a further equilibrium point at $(\boldsymbol{x},\boldsymbol{\theta}) = (\boldsymbol{0},\boldsymbol{\theta}^*)$ where $\boldsymbol{\theta}^* = (\theta_H^*, \theta_V^*)$ has components given by

$$\theta_H^* = \ln\left(\frac{kp+\delta}{kp+\delta R_0}\right), \qquad \theta_V^* = \ln\left(\frac{kcq+\sigma}{kcq+\sigma R_0}\right).$$

To find the value of $U(\boldsymbol{0})$, we solve (numerically) Eqs. (11) along the characteristic curve connecting $(\boldsymbol{x},\boldsymbol{\theta}) = (\boldsymbol{x}^*,\boldsymbol{0})$ at $t = -\infty$ to $(\boldsymbol{x},\boldsymbol{\theta}) = (\boldsymbol{0},\boldsymbol{\theta}^*)$ at $t = +\infty$, and then compute

$$U(\boldsymbol{0}) = \int_{-\infty}^{\infty}\boldsymbol{\theta}^T\frac{d\boldsymbol{x}}{dt}\,dt, \tag{12}$$

the integral being evaluated along the relevant characteristic curve [13]. The value of $U(\boldsymbol{0})$ gives an indication of the expected time to extinction from quasistationarity, τ, via the relationship (9).

2.2. Computational methods

Solving Eqs. (11) subject to $(\boldsymbol{x},\boldsymbol{\theta}) = (\boldsymbol{x}^*,\boldsymbol{0})$ at $t = -\infty$ and $(\boldsymbol{x},\boldsymbol{\theta}) = (\boldsymbol{0},\boldsymbol{\theta}^*)$ at $t = +\infty$ is a boundary value problem, so we use the Matlab function `bvp5c`. We first apply the time transformation $\bar{t} = \tanh\lambda t$. This provides a convenient way to transform the interval $t\in(-\infty,\infty)$ to the finite interval $\bar{t}\in(-1,1)$, with the value of λ being chosen by experiment. For all parameter values that we consider in Section 2.3, the value $\lambda = 1.5$ was found to give good convergence. The `bvp5c` function requires as input an initial guess for the solution trajectory $\{(\boldsymbol{x}(t),\boldsymbol{\theta}(t)) : -\infty < t < \infty\}$. For our initial guess we used a straight line trajectory with points equally spaced in transformed time $\bar{t}$; that is, $\left(\boldsymbol{x}\left(\bar{t}\right),\boldsymbol{\theta}\left(\bar{t}\right)\right) = \left((1-\bar{t})\boldsymbol{x}^*/2, (1+\bar{t})\boldsymbol{\theta}^*/2\right)$.

For a full discussion of the above choices and of alternative computational approaches, see [15].

2.3. Effects of model parameters upon extinction time

To investigate the effects of model parameters upon time to extinction, we vary each parameter in turn while keeping other parameter values fixed at the reference values given in Table 1. From formula (1) we see that the basic reproduction number R_0 is directly proportional to each of the parameters c, p, q, inversely proportional to σ, δ, and proportional to the square of k. We vary each parameter across a range of values such that R_0 varies from 0.75 times its reference value up to 1.25 times the reference value. Results are shown in Fig. 1. The six curves in Fig. 1 all intersect when R_0 is equal to its reference value $R_0 \approx 1.54$, with $U(\boldsymbol{0}) \approx 0.1112$ here. When $R_0 = 1$, we have $U(\boldsymbol{0}) = 0$, and so if the graph were extended to the left we would see all six curves intersect again at the point $(R_0 = 1, U(\boldsymbol{0}) = 0)$.

We see from Fig. 1 that as each parameter is varied, R_0 and $U(\boldsymbol{0})$ (and hence the mean extinction time τ) increase together, but that the rate at which $U(\boldsymbol{0})$ increases depends upon which parameter is being varied. Thus knowledge of the value of R_0 (together with host population size N) is not in itself sufficient to predict extinction time; the values of the individual parameters must be taken into account. For a given change in R_0, we see from Fig. 1 that the parameter with the greatest effect upon the mean extinction time τ is the number of vectors per host, c, followed by the mean vector lifespan, δ^{-1}, the per-bite host to vector transmission probability, q, the biting rate, k, the per-bite vector to host transmission probability, p, and finally the mean host infectious period, σ^{-1}. Note that the form of the relationship (9) implies that small differences in the value of $U(\boldsymbol{0})$ can correspond to large differences in the mean extinction time τ, for even moderate population sizes. So for instance, at the right hand side of Fig. 1, where $R_0 \approx 1.92$, on the curve corresponding to varying the parameter c we have $U(\boldsymbol{0}) \approx 0.2780$, whereas on the curve corresponding to varying σ we have $U(\boldsymbol{0}) \approx 0.2324$. For a host population size of $N = 50$, this corresponds to estimates of τ differing by a factor of approximately 9.8.

These results are largely in line with those set out in Table 2 of [5], with two differences. Firstly, we chose to vary each model

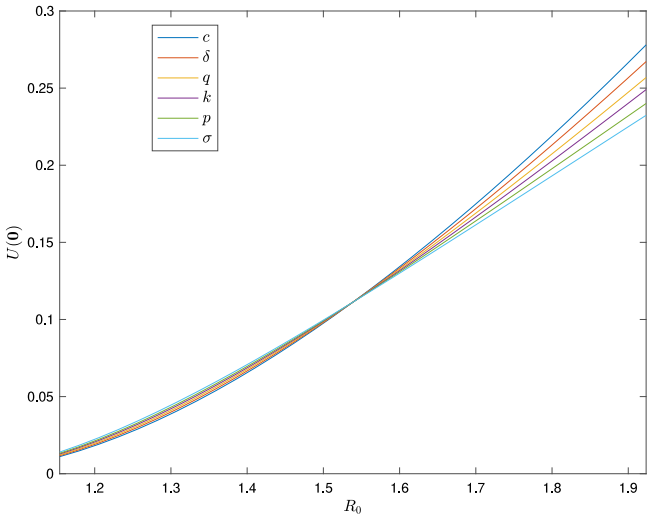

Fig. 1. Plots of $U(\mathbf{0})$ against R_0 for the stochastic Ross–Macdonald model. Each curve shows how $U(\mathbf{0})$ varies with R_0 when a single model parameter is varied while all others remain fixed at the values given in Table 1. Note that $U(\mathbf{0}) = \lim_{N\to\infty} (\ln \tau)/N$, where τ denotes the mean extinction time starting from quasistationarity.

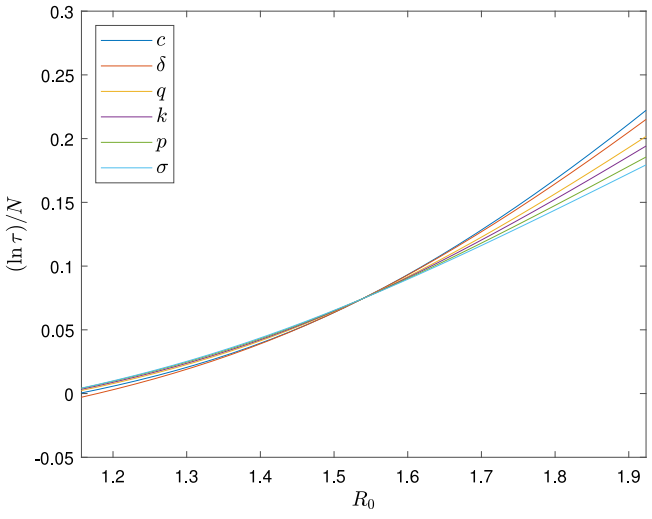

Fig. 2. Plots of $(\ln \tau)/N$ against R_0 for the stochastic Ross–Macdonald model with host population size $N = 50$, where τ denotes the mean extinction time starting from quasistationarity, computed by direct solution of the eigenvalue equation (5). Each curve shows how $(\ln \tau)/N$ varies with R_0 when a single model parameter is varied while all others remain fixed at the values given in Table 1.

parameter to achieve a specified range of R_0 values, whereas in [5] a range was specified for the model parameters themselves; in light of formula (1), this means that our results for the biting rate k are not directly comparable to those of [5]. Secondly, in the results of [5], the ordering of the two least influential parameters, p and σ^{-1}, is reversed compared to our results.

To investigate this discrepancy, for sufficiently small host population size N we can evaluate τ exactly (to machine precision) by direct solution of the eigenvalue equation (5), using the Matlab function `eigs`. Fig. 2 shows results for $N = 50$, with other parameters ranging over the same values as in Fig. 1; we have plotted $(\ln \tau)/N$ to allow direct comparison with Fig. 1. We see that the patterns in Figs. 1 and 2 are very similar, and in particular the ordering of the curves is the same, confirming that the WKB methodology is more reliable than the approach of [5]. However, comparing values on the vertical axes of Figs. 1 and 2, the WKB approach is seen to consistently over-estimate τ. For example, with $N = 50$ and all other parameters taking the reference values given in Table 1, we have $(\ln \tau)/N = 0.0744$, compared to the WKB estimate $U(\mathbf{0}) = 0.1112$. This corresponds to an exact (eigenvalue) result of $\tau = 41.3$ years, compared to a WKB estimate of $\exp(NU(\mathbf{0})) = 260.3$ years, clearly not a very accurate approximation (although still an improvement upon the estimate of 595.4 years given in Table 2 of [5] for these parameter values). Given the form of the asymptotic relationship (9), one would not necessarily expect to obtain very accurate numerical estimates of τ. What one can expect is an indication of how the value of τ changes as parameter values are varied. For instance, at the right hand side of Fig. 2 where $R_0 \approx 1.92$, on the curve corresponding to varying c we have $\tau \approx 7168$ years whereas on the curve corresponding to varying σ we have $\tau \approx 787$ years, so that values of τ differ by a factor of approximately 9.1. This compares well to the previously estimated factor, based on values of $U(\mathbf{0})$ from Fig. 1, of around 9.8.

We next consider the effect of increasing host population size N upon the accuracy of our approximation. Results are shown in Fig. 3, where parameters other than N are fixed at the reference values given in Table 1. As well as results from direct solution of the eigenvalue equation (5), we show simulation results obtained using the discrete event simulation algorithm described in Section 5.4.2 of [16], sometimes referred to as the Doob–Gillespie algorithm. Each simulation run is initiated at time $t = 0$ at the point $\left(\lceil Nx_H^* \rceil, \lceil Nx_V^* \rceil\right)$ where x_H^*, x_V^* are given by the formulae (4), and $\lceil x \rceil$ denotes the least integer greater than or equal to x. The simulation is first run for a burn-in period, to allow the process to (approximately) attain quasistationarity. The time from the end of the burn-in period until disease extinction is recorded. For each value of N, we ran 100 simulations; any runs that went extinct before the end of the burn-in period were re-started from $\left(\lceil Nx_H^* \rceil, \lceil Nx_V^* \rceil\right)$ at time $t = 0$, to ensure a sample of 100 extinction times for each N. The time from quasistationarity to extinction is known to be exponentially distributed, so confidence intervals for τ shown in Fig. 3 were computed using formula (C6) of [17], which is exact for samples from an exponential distribution. A burn-in period of 1 year was found to be sufficient to ensure that the distribution of extinction times is approximately exponentially distributed, for the parameter values of Fig. 3. The time taken to run simulations to extinction increases rapidly with N, and so simulation results were computed only up to $N = 120$. Eigenvalue results were computed up to $N = 200$. For large N, the eigenvalue approach not only becomes more time-consuming (although not to the same extent as simulation), but can also suffer from numerical instability. We were not able to obtain reliable results for N values beyond 200. Note that with $N = 200$ and $c = 5$, the matrix Q_C in Eq. (5) is of size 201200×201200.

We see from Fig. 3 that convergence of $(\ln \tau)/N$ towards $U(\mathbf{0})$ as N increases, predicted by the relationship (9), is rather slow. With $N = 200$, for these parameter values, direct eigenvalue computation gives $(\ln \tau)/N = 0.0978$, compared to the WKB approximation $U(\mathbf{0}) = 0.1112$. That is, the WKB method here over-estimates τ by a factor of $\exp(200\times(0.1112-0.0978)) = 14.6$. We thus see that although the WKB method can accurately reveal the effects of varying different parameter values upon extinction time (as shown by Figs. 1 and 2), the numerical estimates of τ produced are far from accurate.

In the computations for Fig. 1, the initial guess that we supplied to the `bvp5c` function was a straight line trajectory from $(\boldsymbol{x}^*, \mathbf{0})$ to $(\mathbf{0}, \boldsymbol{\theta}^*)$. This works well here because, for R_0 not too far above 1, the true characteristic curve from $(\boldsymbol{x}^*, \mathbf{0})$ to $(\mathbf{0}, \boldsymbol{\theta}^*)$ satisfying Eqs. (11) is not far from a straight line. This suggests that we can approximate $U(\mathbf{0})$ by evaluating the integral on the right hand side of Eq. (12) along the appropriate straight line. Doing so yields the simple explicit approximation $U(\mathbf{0}) \approx \tilde{U}$, where

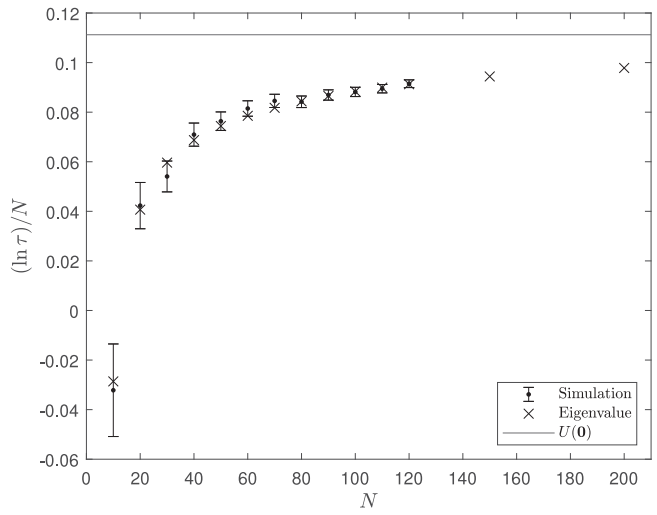

Fig. 3. Plots of $(\ln\tau)/N$ against host population size N for the stochastic Ross–Macdonald model with all other parameter values as given in Table 1, where τ denotes the mean extinction time starting from quasistationarity. Simulation results based on 100 simulations for each value of N, with sample means (dots) and 95% confidence intervals shown; crosses based on values of τ computed by solution of the eigenvalue equation (5); horizontal line shows the value of $U(\mathbf{0})$ computed using WKB methodology.

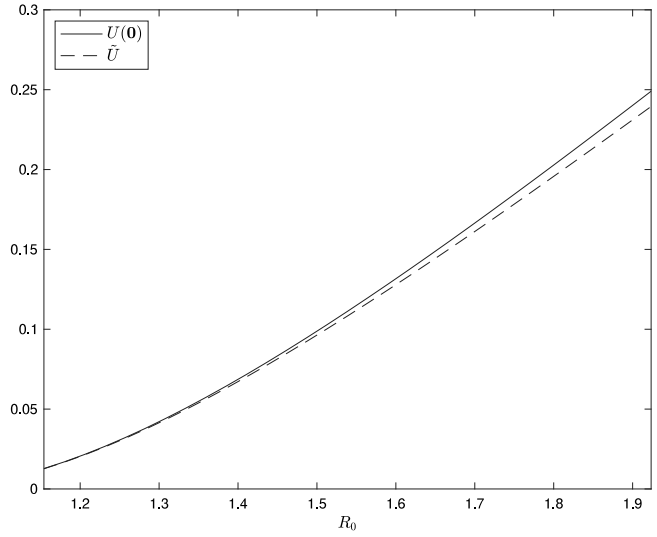

Fig. 4. Plot of $U(\mathbf{0})$ given by Eq. (12) and its approximation $\tilde{U}$ given by Eq. (13) against R_0 for the stochastic Ross–Macdonald model. The biting rate k is varied to achieve the range of R_0 values indicated, while other parameters remain fixed at their reference values given in Table 1.

$$\begin{aligned}\tilde{U} &= -\frac{1}{2}\boldsymbol{x}^{*T}\boldsymbol{\theta}^{*}\\ &= \frac{(R_0-1)\,kc}{2R_0}\left(\frac{p}{kpc+\sigma}\ln\left(1+\frac{\delta(R_0-1)}{kp+\delta}\right)\right.\\ &\qquad\left.+\frac{q}{kq+\delta}\ln\left(1+\frac{\sigma(R_0-1)}{kcq+\sigma}\right)\right).\end{aligned}\tag{13}$$

The true value $U(\mathbf{0})$ is plotted alongside its approximation $\tilde{U}$ in Fig. 4, where the biting rate parameter k is varied across the same range as for Fig. 1 while other parameters remain fixed at their reference values given in Table 1. We see that $\tilde{U}$ provides a good approximation to $U(\mathbf{0})$ for R_0 values not too much greater than 1, although the error in the approximation grows as R_0 increases, and we should bear in mind that, in light of the relationship (9), small errors in the value of $U(\mathbf{0})$ can correspond to large errors in our estimate of the mean extinction time τ.

Table 3
Transition rates for the stochastic Ross–Macdonald model in a heterogeneous population.

Event	State transition	Transition rate
Infection of a host of type i	$Y_{Hi} \to Y_{Hi}+1$	$\left(\left(H_i - Y_{Hi}\right)/H_i\right)\sum_{r=1}^{n} Y_{Vr}\alpha_{ri}$
Infection of a vector of type r	$Y_{Vr} \to Y_{Vr}+1$	$\left(V_r - Y_{Vr}\right)\sum_{i=1}^{m}\left(Y_{Hi}/H_i\right)\beta_{ir}$
Recovery of a host of type i	$Y_{Hi} \to Y_{Hi}-1$	$\sigma_i Y_{Hi}$
Death of a vector of type r	$Y_{Vr} \to Y_{Vr}-1$	$\delta_r Y_{Vr}$

3. The effects of heterogeneities

3.1. The heterogeneous population model

We extend the model of Section 2 to allow heterogeneity in both hosts and vectors as follows, following [4,8]. Let m denote the number of types of host and n the number of types of vector. For $i = 1,2,\dots,m$, denote by H_i the (constant) number of hosts of type i and by Y_{Hi} the number of infected hosts of type i, set $N = \sum_{i=1}^{m} H_i$ to be the total size of the host population, and denote by $h_i = H_i/N$ the proportion of hosts that are of type i. For $r = 1,2,\dots,n$, denote by V_r the (constant) number of vectors of type r and by Y_{Vr} the number of infected vectors of type r, set $V = \sum_{r=1}^{n} V_r$ to be the total size of the vector population, and denote by $v_r = V_r/V$ the proportion of vectors that are of type r. Define $c = V/N$ to be the overall number of vectors per host. For $i = 1,2,\dots,m$, $r = 1,2,\dots,n$, the parameter governing the rate of transmission from infected vectors of type r to susceptible hosts of type i is $\alpha_{ri} = k_r\gamma_{ri}p_{ri}$, where k_r is the biting rate of type r vectors, γ_{ri} is the probability that a bite by a type r vector is on a type i host (so $\sum_{i=1}^{m}\gamma_{ri} = 1$ for $r = 1,2,\dots,n$), and p_{ri} is the probability of such a bite leading to transmission if the vector is infected and the host susceptible. Similarly, the parameter governing the rate of transmission from infected hosts of type i to susceptible vectors of type r is $\beta_{ir} = k_r\gamma_{ri}q_{ir}$, where q_{ir} is the probability of a bite from a susceptible type r vector on an infected type i host leading to transmission. Denote by σ_i the recovery rate of hosts of type i for $i = 1,2,\dots,m$, and by δ_r the death rate of infected vectors of type r for $r = 1,2,\dots,n$. We assume throughout that $h_i,\sigma_i,v_r,\delta_r,k_r > 0$ for $i = 1,2,\dots,m$, $r = 1,2,\dots,n$. We further assume, following [8,18], that for each $i \in \{1,2,\dots,m\}$, $r \in \{1,2,\dots,n\}$, we have $p_{ri} \neq 0$ if and only if $q_{ir} \neq 0$, and that the system is *connected*, in the sense that for each $i \in \{1,2,\dots,m\}$, $r \in \{1,2,\dots,n\}$ it is possible for infection to be transmitted between host type i and vector type r, either directly or via some intermediate chain of host and vector types. Writing $\boldsymbol{Y}(t) = (Y_{H1}(t),Y_{H2}(t),\dots,Y_{Hm}(t),Y_{V1}(t),Y_{V2}(t),\dots,Y_{Vn}(t))$ then the process $\{\boldsymbol{Y}(t) : t \geq 0\}$ is a Markov process with transition rates given in Table 3.

The model of [8] is obtained by setting $\sigma_i = \sigma$, $\delta_r = \delta$, $k_r = k$, $p_{ri} = p$ and $q_{ir} = q$ for $i = 1,2,\dots,m$, $r = 1,2,\dots,n$. That is, there is assumed in [8] to be a common recovery rate σ for all host types, a common death rate δ for all vector types, a common biting rate k for all vector types, and that transmission probabilities p_{ri}, q_{ir} do not depend upon the type of the host or vector. The heterogeneity then lies entirely in the vector biting preference parameters $\{\gamma_{ri} : i = 1,2,\dots,m,\ r = 1,2,\dots,n\}$.

Denote by a_{ij} the average number of secondary infections that arise among hosts of type j from an infected host of type i introduced into an entirely susceptible population. Then we have [4] that for $i,j = 1,2,\dots,m$,

$$a_{ij} = \frac{c}{h_i\sigma_i}\sum_{r=1}^{n}\frac{\beta_{ir}v_r\alpha_{rj}}{\delta_r}.$$

It follows from our assumptions that the host-to-host next generation matrix A with entries $\{a_{ij} : i,j = 1,2,\dots,m\}$ is irreducible [8]. The host-to-host basic reproduction number R_0 is given by the Perron–Frobenius eigenvalue of A.

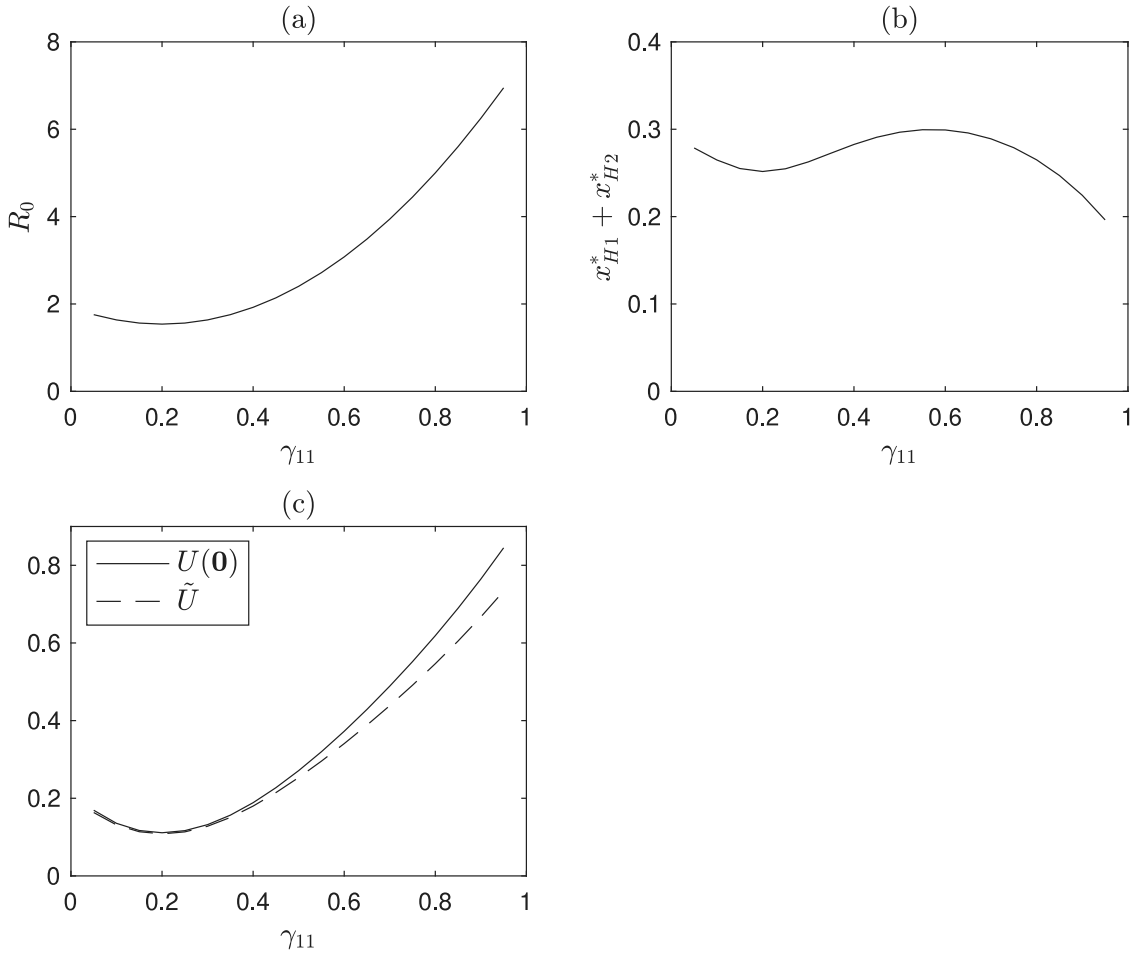

Fig. 5. For the stochastic Ross–Macdonald model in a heterogeneous population with $m = 2$ host types and $n = 1$ vector type, plots of (a) basic reproduction number R_0; (b) deterministic endemic prevalence level amongst hosts, $x^*_{H1} + x^*_{H2}$; (c) $U(\mathbf{0}) = \lim_{N\to\infty}(\ln \tau)/N$ and its approximation $\tilde{U}$, where τ is the expected time to extinction starting from quasistationarity. Each quantity plotted against the biting preference parameter γ_{11}, with $\gamma_{12} = 1 - \gamma_{11}$, $(h_1, h_2) = (0.2, 0.8)$, and other parameter values as given in Table 1.

The scaled process $\frac{1}{N}\left(Y_{H1}, Y_{H2}, \ldots, Y_{Hm}, Y_{V1}, Y_{V2}, \ldots, Y_{Vn}\right)$ may be approximated, for large N, by the solution $\boldsymbol{x} = \left(x_{H1}, x_{H2}, \ldots, x_{Hm}, x_{V1}, x_{V2}, \ldots, x_{Vn}\right)$ to the following deterministic system, extending system (3).

$$\left.\begin{aligned} \frac{dx_{Hi}}{dt} &= \left(1 - \frac{x_{Hi}}{h_i}\right)\sum_{r=1}^{n} x_{Vr}\alpha_{ri} - \sigma_i x_{Hi} \text{ for } i = 1, 2, \ldots, m, \\ \frac{dx_{Vr}}{dt} &= (cv_r - x_{Vr})\sum_{i=1}^{m} \frac{x_{Hi}}{h_i}\beta_{ir} - \delta_r x_{Vr} \text{ for } r = 1, 2, \ldots, n. \end{aligned}\right\} \tag{14}$$

The deterministic system (14) has an equilibrium point at $\boldsymbol{x} = \mathbf{0}$, the disease free state. It is shown in [8] that either (i) the disease-free state is the only feasible equilibrium and is stable; or (ii) there is one other feasible equilibrium point $\boldsymbol{x}^*$, and the point $\boldsymbol{x}^*$ is stable while the disease-free equilibrium is unstable ([8] Appendix A, remark following proof of theorem 7). In the case that $\sigma_i = \sigma$, $\delta_r = \delta$, $k_r = k$, $p_{ri} = p$ and $q_{ir} = q$ for $i = 1, 2, \ldots, m$, $r = 1, 2, \ldots, n$, it is further shown that case (i) occurs if $R_0 \le 1$ and case (ii) if $R_0 > 1$ ([8] Appendix A, theorem 8).

Applying the WKB *ansatz* as in Section 2, the Hamiltonian corresponding to the heterogeneous population model with transition rates given in Table 3 is

$$\begin{aligned} H(\boldsymbol{x}, \boldsymbol{\theta}) = &\sum_{i=1}^{m}\sum_{r=1}^{n} x_{Vr}\alpha_{ri}\left(1 - \frac{x_{Hi}}{h_i}\right)\left(\mathrm{e}^{\theta_{Hi}} - 1\right) \\ &+ \sum_{i=1}^{m}\sum_{r=1}^{n} \frac{x_{Hi}}{h_i}\beta_{ir}(cv_r - x_{Vr})\left(\mathrm{e}^{\theta_{Vr}} - 1\right) \\ &+ \sum_{i=1}^{m} \sigma_i x_{Hi}\left(\mathrm{e}^{-\theta_{Hi}} - 1\right) + \sum_{r=1}^{n} \delta_r x_{Vr}\left(\mathrm{e}^{-\theta_{Vr}} - 1\right), \end{aligned} \tag{15}$$

where $\boldsymbol{\theta} = \left(\theta_{H1}, \theta_{H2}, \ldots, \theta_{Hm}, \theta_{V1}, \theta_{V2}, \ldots, \theta_{Vn}\right)$.

The characteristic ordinary differential Eqs. (10) for this model are presented in Appendix, Eqs. (A.1). Setting $\boldsymbol{\theta} = \mathbf{0}$ in Eqs. (A.1) we recover Eqs. (14), with equilibrium points at $(\boldsymbol{x}, \boldsymbol{\theta}) = (\mathbf{0}, \mathbf{0})$ and $(\boldsymbol{x}, \boldsymbol{\theta}) = (\boldsymbol{x}^*, \mathbf{0})$. Setting $\boldsymbol{x} = \mathbf{0}$ in Eqs. (A.1) we find that the point $(\boldsymbol{x}, \boldsymbol{\theta}) = \left(\mathbf{0}, \boldsymbol{\theta}^*\right)$ is an equilibrium point if the components of $\boldsymbol{\theta}^* = \left(\theta^*_{H1}, \theta^*_{H2}, \ldots, \theta^*_{Hm}, \theta^*_{V1}, \theta^*_{V2}, \ldots, \theta^*_{Vn}\right)$ satisfy

$$\left.\begin{aligned} h_i\sigma_i\left(\mathrm{e}^{-\theta_{Hi}} - 1\right) + \sum_{r=1}^{n} c\beta_{ir}v_r\left(\mathrm{e}^{\theta_{Vr}} - 1\right) &= 0 \text{ for } i = 1, 2, \ldots, m, \\ \delta_r\left(\mathrm{e}^{-\theta_{Vr}} - 1\right) + \sum_{i=1}^{m} \alpha_{ri}\left(\mathrm{e}^{\theta_{Hi}} - 1\right) &= 0 \text{ for } r = 1, 2, \ldots, n. \end{aligned}\right\} \tag{16}$$

Solving Eqs. (A.1) numerically along tbe characteristic curve connecting $(\boldsymbol{x}, \boldsymbol{\theta}) = (\boldsymbol{x}^*, \mathbf{0})$ at $t = -\infty$ to $(\boldsymbol{x}, \boldsymbol{\theta}) = (\mathbf{0}, \boldsymbol{\theta}^*)$ at $t = +\infty$ and then computing $U(\mathbf{0})$ from Eq. (12) gives an indication of the expected time to extinction from quasistationarity, τ, via the relationship (9).

3.2. Computational methods

As in Section 2, we use the Matlab function `bvp5c` to solve Eqs. (A.1), after first applying the time transformation $\bar{t} = \tanh \lambda t$, and using as initial guess the straight line trajectory from $(\boldsymbol{x}^*, \mathbf{0})$ to $(\mathbf{0}, \boldsymbol{\theta}^*)$. Taking a single value for the parameter λ did not give satisfactory convergence for all model parameter values considered, so instead the

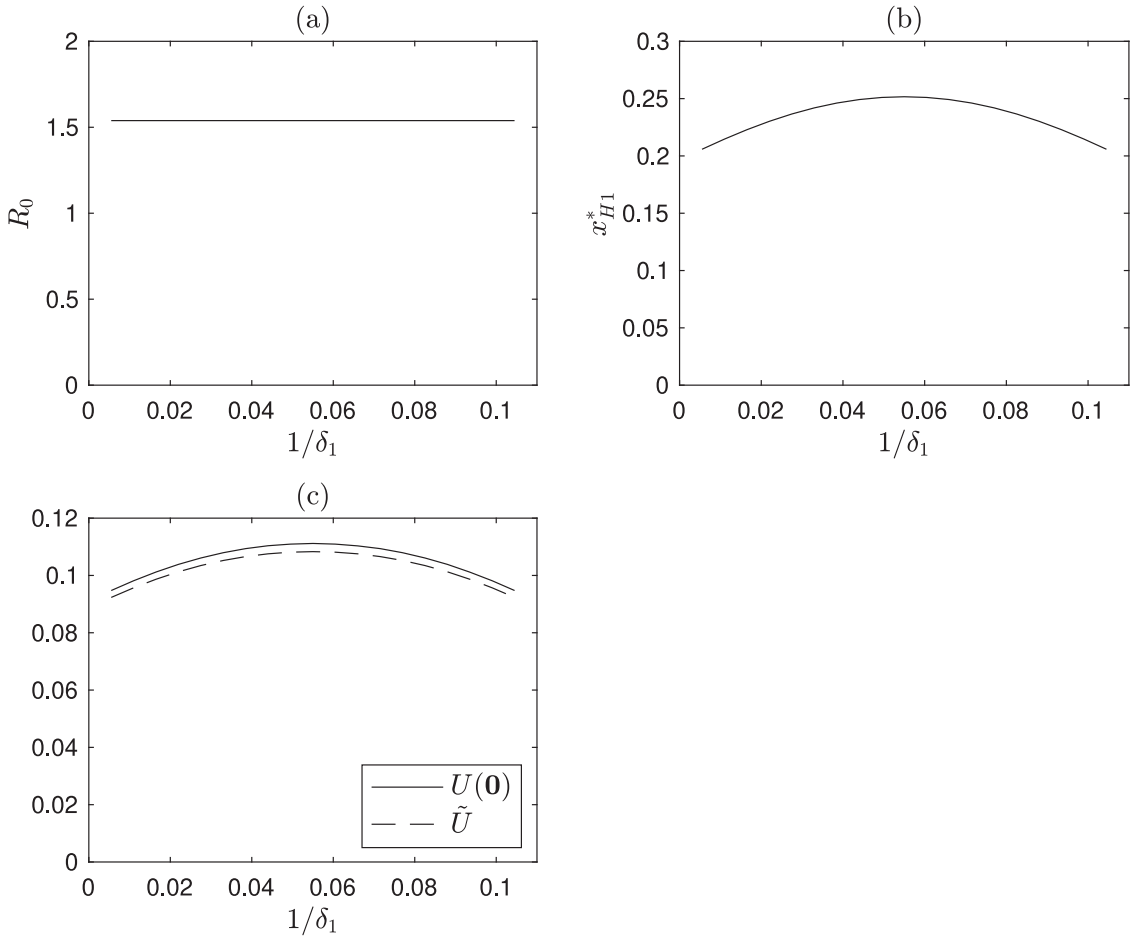

Fig. 6. For the stochastic Ross–Macdonald model in a heterogeneous population with $m = 1$ host type and $n = 2$ vector types, plots of (a) basic reproduction number R_0; (b) deterministic endemic prevalence level amongst hosts, x^*_{H1}; (c) $U(\mathbf{0}) = \lim_{N\to\infty}(\ln \tau)/N$ and its approximation $\tilde{U}$, where τ is the expected time to extinction starting from quasistationarity. Each quantity plotted against the mean lifespan of type 1 vectors, δ_1^{-1}, with the overall mean lifespan of vectors $(\upsilon_1/\delta_1) + (\upsilon_2/\delta_2)$ held constant and equal to $1/\delta = 0.055$, $(\upsilon_1, \upsilon_2) = (0.5, 0.5)$, other parameter values as given in Table 1.

value of λ is taken to be of the form $\lambda = \lambda'\sqrt{\boldsymbol{x}^{*T}\boldsymbol{x}^* + \boldsymbol{\theta}^{*T}\boldsymbol{\theta}^*}$, a multiple of the straight line distance from $(\boldsymbol{x}^*, \mathbf{0})$ to $(\mathbf{0}, \boldsymbol{\theta}^*)$. The value of λ' was chosen by experiment; specifically, we took $\lambda' = 3$ to compute Figs. 5 and 7, and $\lambda' = 4$ for Fig. 6. The equations for the equilibrium points $\boldsymbol{x}^*$ and $\boldsymbol{\theta}^*$ also now need to be solved numerically. In the case $m > 1$ and $n > 1$ (Section 3.5), we use the Matlab function `fsolve` to solve the $m + n$ dimensional systems satisfied by $\boldsymbol{x}^*$ and $\boldsymbol{\theta}^*$. For the cases $n = 1$ (Section 3.3) and $m = 1$ (Section 3.4) we instead use the Matlab function `fzero` to solve the 1 dimensional systems (18), (20) and (24), (26).

In computing Fig. 2, where $N = 50$ and $c = 5$ (except for the curve along which c is varied), the matrix Q_C was of size $12\,800 \times 12\,800$. If, for example, both hosts and vectors are split into two equally sized groups, so that $m = n = 2$ and $h_1 = h_2 = \upsilon_1 = \upsilon_2 = 0.5$, and we again take $N = 50$ and $c = 5$, then the matrix Q_C is now of size $10\,732\,175 \times 10\,732\,175$. We can see that, other than for very small population sizes, solving the eigenvalue equation (5) using the Matlab function `eigs` is impractical for the heterogeneous population model. We could attempt to estimate τ through simulation, as in Fig. 3, but this requires many simulation runs for each set of parameter values, and the time taken to run each simulation to extinction increases rapidly with population size, as well as increasing with τ. Consequently, for the heterogeneous population model we present only results based on the WKB approximation.

3.3. One vector type, many host types

In the case of a single vector type, so $n = 1$, the host-to-host next generation matrix A is separable; that is to say, it may be written in the form $A = \boldsymbol{a}\boldsymbol{b}^T$ for appropriate column vectors $\boldsymbol{a}, \boldsymbol{b}$. The Perron–Frobenius eigenvalue of A in this case is $\boldsymbol{b}^T\boldsymbol{a}$, and so the basic reproduction number is given [4] by

$$R_0 = \frac{c}{\delta_1}\sum_{i=1}^{m}\frac{\beta_{i1}\alpha_{1i}}{h_i\sigma_i}.$$

The endemic equilibrium point $\boldsymbol{x}^*$ of the deterministic system (14) has components given (see Appendix of [7]) by

$$x^*_{Hi} = \frac{h_i\alpha_{1i}x^*_{V1}}{h_i\sigma_i + \alpha_{1i}x^*_{V1}} \text{ for } i = 1, 2, \ldots, m, \tag{17}$$

where x^*_{V1} satisfies

$$\frac{1}{\delta_1}\sum_{i=1}^{m}\frac{\beta_{i1}\alpha_{1i}\left(c - x^*_{V1}\right)}{h_i\sigma_i + \alpha_{1i}x^*_{V1}} = 1. \tag{18}$$

The left hand side of Eq. (18) is a continuous, decreasing function of x^*_{V1} on the interval $[0, c]$, and is equal to R_0 at the left hand end of the interval, zero at the right hand end of the interval. Hence for $R_0 > 1$, Eq. (18) has a unique solution $x^*_{V1} \in (0, c)$. Having solved Eq. (18) numerically for x^*_{V1}, the corresponding values of $x^*_{H1}, x^*_{H2}, \ldots, x^*_{Hn}$ may be computed from Eqs. (17).

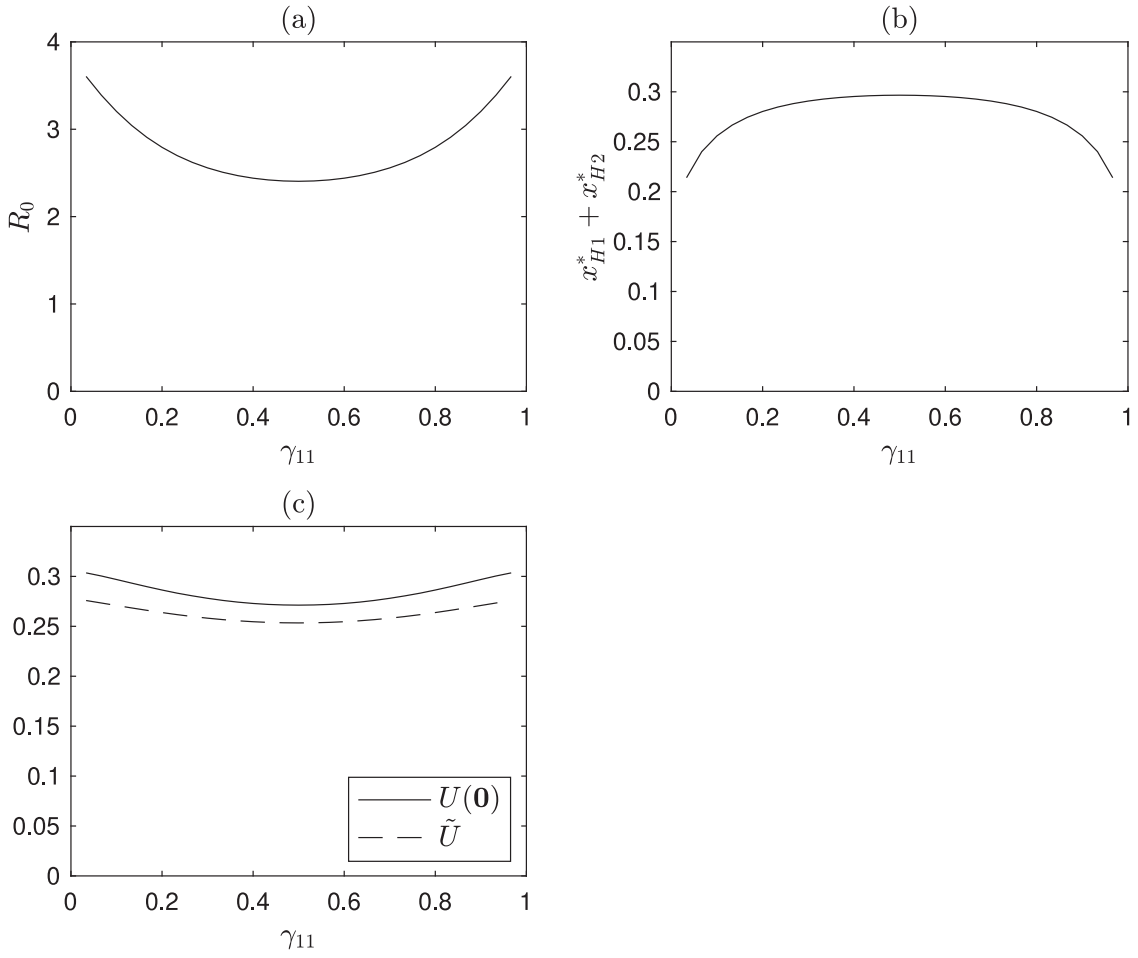

Fig. 7. For the stochastic Ross–Macdonald model in a heterogeneous population with $m = 2$ host types and $n = 2$ vector types, plots of (a) basic reproduction number R_0; (b) deterministic endemic prevalence level amongst hosts, $x^*_{H1} + x^*_{H2}$; (c) $U(\mathbf{0}) = \lim_{N\to\infty}(\ln \tau)/N$ and its approximation $\tilde{U}$, where τ is the expected time to extinction starting from quasistationarity. Each quantity plotted against the biting preference parameter γ_{11}, with $\gamma_{12} = 1 - \gamma_{11}$, the overall proportion of bites that are on type 1 hosts, $v_1\gamma_{11} + v_2\gamma_{21}$, held constant and equal to v_1, $\gamma_{22} = 1 - \gamma_{21}$, $(h_1, h_2) = (0.2, 0.8)$, $(v_1, v_2) = (0.5, 0.5)$, and other parameter values as given in Table 1.

From Eqs. (16) with $n = 1$, any equilibrium point of the characteristic ordinary differential Eqs. (A.1) of the form $(\boldsymbol{x}, \boldsymbol{\theta}) = (\mathbf{0}, \boldsymbol{\theta}^*)$ with $\boldsymbol{\theta}^* \neq \mathbf{0}$ has components given by

$$\theta^*_{Hi} = -\ln\left(1 + \frac{c\beta_{i1}}{h_i\sigma_i}\left(1 - \mathrm{e}^{\theta^*_{V1}}\right)\right) \text{ for } i = 1, 2, \ldots, m, \tag{19}$$

where θ^*_{V1} satisfies

$$\frac{c}{\delta_1}\sum_{i=1}^{m}\frac{\beta_{i1}\alpha_{1i}\mathrm{e}^{\theta^*_{V1}}}{h_i\sigma_i + c\beta_{i1}\left(1 - \mathrm{e}^{\theta^*_{V1}}\right)} = 1. \tag{20}$$

From Eqs. (19), in order to obtain real solutions for $\theta^*_{H1}, \theta^*_{H2}, \ldots, \theta^*_{Hm}$, we require $\theta^*_{V1} < \ln\left(1 + \left(h_i\sigma_i/(c\beta_{i1})\right)\right)$ for $i = 1, 2, \ldots, m$. Setting

$$\tilde{\theta}_V = \min\left\{\ln\left(1 + \left(h_i\sigma_i/(c\beta_{i1})\right)\right) : i = 1, 2, \ldots, m\right\},$$

then $\tilde{\theta}_V > 0$, and the left hand side of Eq. (20) is a continuous, increasing function of θ^*_{V1} on the interval $(-\infty, \tilde{\theta}_V)$, tending to zero as $\theta^*_{V1} \to -\infty$ and taking the value R_0 when $\theta^*_{V1} = 0$. Consequently, for $R_0 > 1$ Eq. (20) has a unique solution θ^*_{V1} in the interval $(-\infty, \tilde{\theta}_V)$, and $\theta^*_{V1} < 0$. Once we have found the value of θ^*_{V1} from Eq. (20), then Eqs. (19) may be used to find $\theta^*_{H1}, \theta^*_{H2}, \ldots, \theta^*_{Hm}$. Observe that $\theta^*_{V1} < 0$ implies $\theta^*_{Hi} < 0$ for $i = 1, 2, \ldots, m$.

To investigate the effect of heterogeneous biting preferences upon extinction time, we consider a population with $m = 2$ host types and $n = 1$ vector type, in which hosts differ only in terms of their attractiveness to vectors. We take 20% of hosts to be of type 1, so $(h_1, h_2) = (0.2, 0.8)$. With values of $c, k, p, q, \sigma, \delta$ as in Table 1, we set $\sigma_1 = \sigma_2 = \sigma$, $\delta_1 = \delta$, $k_1 = k$, $p_{11} = p_{12} = p$ and $q_{11} = q_{21} = q$. The parameter γ_{11} specifies the proportion of bites that are upon hosts of type 1 (and recall that $\gamma_{12} = 1 - \gamma_{11}$), so that the value $\gamma_{11} = h_1 = 0.2$ corresponds to homogeneous mixing.

Fig. 5 illustrates the effect of varying the biting preference parameter γ_{11} upon: (a) the basic reproduction number R_0; (b) the overall endemic equilibrium prevalence amongst hosts in the deterministic model $\sum_{i=1}^{m} x^*_{Hi}$; and (c) $U(\mathbf{0}) = \lim_{N\to\infty}(\ln \tau)/N$, where τ is the mean persistence time starting from quasistationarity. In this scenario, we have

$$R_0 = \frac{cpqk^2}{\sigma\delta}\left(\frac{\gamma_{11}^2}{h_1} + \frac{\gamma_{12}^2}{h_2}\right) = \frac{cpqk^2}{\sigma\delta}\left(\frac{\gamma_{11}^2}{h_1} + \frac{(1-\gamma_{11})^2}{1-h_1}\right),$$

so that, as pointed out in [7], R_0 is a quadratic function of γ_{11}, minimised for the homogeneous case $\gamma_{11} = h_1 = 0.2$, and we see this in Fig. 5(a). It was also remarked in [7] that non-homogeneous biting preferences can increase or decrease endemic prevalence amongst hosts in the deterministic model, and we observe this effect in Fig. 5(b). However, we see from Fig. 5(c) that the value of $U(\mathbf{0}) = \lim_{N\to\infty}(\ln \tau)/N$ is minimised when $\gamma_{11} = 0.2$, so that for these parameter values, heterogeneity in biting preference can only increase the expected disease persistence time. It is interesting to note that for high values of γ_{11}, as γ_{11} increases, the endemic prevalence level of the deterministic model decreases while the expected disease persistence time increases. This can be explained if the decrease in endemic prevalence level is more than counterbalanced by a reduction in variability, so that stochastic

fluctuations leading to extinction become rarer. Such a reduction in variability has indeed been observed, see Fig. 7 of [4].

As in Section 2, we can approximate $U(\mathbf{0})$ by evaluating the integral in (12) along a straight line trajectory from $(\boldsymbol{x}^*, \mathbf{0})$ to $(\mathbf{0}, \boldsymbol{\theta}^*)$ to give the approximation $U(\mathbf{0}) \approx \tilde{U} = -\boldsymbol{x}^{*T}\boldsymbol{\theta}^*/2$. From Eqs. (17), (19) we find

$$\tilde{U} = -\frac{1}{2}x^*_{V1}\theta^*_{V1} + \frac{1}{2}\sum_{i=1}^{m}\left(\frac{h_i\alpha_{i1}x^*_{V1}}{h_i\sigma_i + \alpha_{1i}x^*_{V1}}\right)\ln\left(1 + \frac{c\beta_{i1}}{h_i\sigma_i}\left(1 - \mathrm{e}^{\theta^*_{V1}}\right)\right), \quad (21)$$

where x^*_{V1}, θ^*_{V1} are given by Eq. (18), (20), respectively. Fig. 5(c) shows the approximation $\tilde{U}$ alongside the true value $U(\mathbf{0})$. From Fig. 5(a) and (c) we see that, as in the homogeneous case, $\tilde{U}$ provides a good approximation to $U(\mathbf{0})$ for R_0 values not too far above 1.

3.4. One host type, many vector types

When heterogeneity is in biting preferences only, then as pointed out in [7], there is no difference between the model with a single host type ($m = 1$) and $n > 1$ vector types and the homogeneous ($m = n = 1$) model, since we necessarily have $\gamma_{r1} = 1$ for $r = 1, 2, \ldots, n$. On the other hand, heterogeneity in biting rates k_r and vector death rates δ_r may be relevant. For instance, malaria is spread by a number of different species of *Anopheles* mosquito, with literature estimates of mean lifespan differing between species [6].

In the case that there is only $m = 1$ type of host, the host-to-host next generation matrix A is a 1×1 matrix, with the basic reproduction number being given by

$$R_0 = \frac{c}{\sigma_1}\sum_{r=1}^{n}\frac{\beta_{1r}\upsilon_r\alpha_{r1}}{\delta_r}. \quad (22)$$

The endemic equilibrium point $\boldsymbol{x}^*$ of the deterministic system (14) has components given by

$$x^*_{Vr} = \frac{c\beta_{1r}\upsilon_r x^*_{H1}}{\delta_r + \beta_{1r}x^*_{H1}} \text{ for } r = 1, 2, \ldots, n, \quad (23)$$

where x^*_{H1} satisfies

$$\frac{c}{\sigma_1}\sum_{r=1}^{n}\frac{\beta_{1r}\upsilon_r\alpha_{r1}\left(1 - x^*_{H1}\right)}{\delta_r + \beta_{1r}x^*_{H1}} = 1. \quad (24)$$

By similar arguments to those following Eq. (18), we find that for $R_0 > 1$, Eq. (24) has a unique solution $x^*_{H1} \in (0, 1)$. Having solved Eq. (24) for x^*_{H1}, the corresponding values of $x^*_{V1}, x^*_{V2}, \ldots, x^*_{Vn}$ may be computed from Eqs. (23).

From Eqs. (16) with $m = 1$ we find that any equilibrium point of Eqs. (A.1) of the form $(\boldsymbol{x}, \boldsymbol{\theta}) = (\mathbf{0}, \boldsymbol{\theta}^*)$ with $\boldsymbol{\theta}^* \neq \mathbf{0}$ has components given by

$$\theta^*_{Vr} = -\ln\left(1 + \frac{\alpha_{r1}}{\delta_r}\left(1 - \mathrm{e}^{\theta^*_{H1}}\right)\right) \text{ for } r = 1, 2, \ldots, n, \quad (25)$$

where θ^*_{H1} satisfies

$$\frac{c}{\sigma_1}\sum_{r=1}^{n}\frac{\beta_{1r}\upsilon_r\alpha_{r1}\mathrm{e}^{\theta^*_{H1}}}{\delta_r + \alpha_{r1}\left(1 - \mathrm{e}^{\theta^*_{H1}}\right)} = 1. \quad (26)$$

By similar arguments to those following Eq. (20), we find that for $R_0 > 1$, Eq. (26) has a unique solution θ^*_{H1} corresponding to real solutions $\theta^*_{V1}, \theta^*_{V2}, \ldots, \theta^*_{Vn}$ to Eqs. (25), and that $\theta^*_{H1}, \theta^*_{V1}, \theta^*_{V2}, \ldots, \theta^*_{Vn} < 0$.

We can again approximate $U(\mathbf{0})$ by evaluating the integral in (12) along a straight line trajectory from $(\boldsymbol{x}^*, \mathbf{0})$ to $(\mathbf{0}, \boldsymbol{\theta}^*)$ to give the approximation $U(\mathbf{0}) \approx \tilde{U} = -\boldsymbol{x}^{*T}\boldsymbol{\theta}^*/2$. From Eqs. (23), (25) we find

$$\tilde{U} = -\frac{1}{2}x^*_{H1}\theta^*_{H1} + \frac{1}{2}\sum_{i=1}^{m}\left(\frac{c\beta_{1r}\upsilon_r x^*_{H1}}{\delta_r + \beta_{1r}x^*_{H1}}\right)\ln\left(1 + \frac{\alpha_{r1}}{\delta_r}\left(1 - \mathrm{e}^{\theta^*_{H1}}\right)\right), \quad (27)$$

where x^*_{H1}, θ^*_{H1} are given by Eqs. (24), (26), respectively.

We consider the effect of heterogeneity in vector lifespans for a population with $m = 1$ host type and $n = 2$ vector types. We take 50% of vectors to be of each type, so $(\upsilon_1, \upsilon_2) = (0.5, 0.5)$. With values of $c, k, p, q, \sigma, \delta$ as in Table 1, we set $k_1 = k_2 = k$, $p_{11} = p_{21} = p$, $q_{11} = q_{12} = q$, and vary δ_1 while keeping fixed the overall mean vector lifespan $(\upsilon_1/\delta_1) + (\upsilon_2/\delta_2) = 1/\delta = 0.055$. The value $\delta_1^{-1} = 0.055$ then corresponds to homogeneous mixing.

Fig. 6 illustrates the effect of varying the mean lifespan δ_1^{-1} of type 1 vectors, while keeping fixed the overall mean vector lifespan $(\upsilon_1/\delta_1) + (\upsilon_2/\delta_2)$, upon: (a) the basic reproduction number R_0; (b) the overall endemic equilibrium prevalence amongst hosts in the deterministic model x^*_{H1}; and (c) $U(\mathbf{0}) = \lim_{N\to\infty}(\ln\tau)/N$, where τ is the mean persistence time starting from quasistationarity. Since the overall mean vector lifespan $(\upsilon_1/\delta_1) + (\upsilon_2/\delta_2)$ is kept fixed, the value of R_0, given by formula (22), remains constant and equal to its reference value $R_0 \approx 1.54$, as we see in Fig. 6(a). Fig. 6(b), (c) show that both the endemic prevalence level in the deterministic model, x^*_{H1}, and expected persistence time starting from quasistationarity, τ, are maximised in the homogeneous ($\delta_1^{-1} = 0.055$) case. This is in contrast to what we observed in Section 3.3 and in Fig. 5, with heterogeneity in biting preferences, where expected persistence time was minimised in the homogeneous case, and the endemic prevalence level could be either higher or lower than in the homogeneous case. Note that for each of the plots in Fig. 6, reflection about the line $\delta_1^{-1} = 0.055$ amounts to simply interchanging the labelling of the two vector types, hence the symmetry we observe in Fig. 6(b), (c). From Fig. 6(c) we see that $\tilde{U}$ provides quite a good approximation to $U(\mathbf{0})$ regardless of the value of δ_1, reflecting the fact that the approximation $\tilde{U}$ generally seems good for values of R_0 not too far above 1, and the value of R_0 is not varying here.

3.5. Many host types and many vector types

For the case of $m > 1$ host types and $n > 1$ vector types, we consider a scenario in which heterogeneity exists only in vector biting preferences, extending the model of Section 3.3. We follow [8] by comparing the model with biting preference parameters $\{\gamma_{ri} : r = 1, 2, \ldots, n,\ i = 1, 2, \ldots, m\}$ to the model with m host types, 1 vector type, and biting preference parameters given by $\bar{\gamma}_{1i} = \sum_{r=1}^{n}\upsilon_r\gamma_{ri}$ for $i = 1, 2, \ldots, n$, thereby holding fixed the proportion of all bites that are on hosts of type i. Denoting by $R_0(m/n)$ the basic reproduction number of the model with m host types and n vector types, and by $R_0(m/1)$ the basic reproduction number of the corresponding model with m host types and 1 vector type (with biting preference parameters $\bar{\gamma}_{1i}$), then [8] showed that $R_0(m/n) \geq R_0(m/1) \geq R_0(1/1)$. Moreover, it was demonstrated in [8] that strong associations between particular groups of vectors and hosts lead to higher R_0 values than non-homogeneous host selection by vectors alone, and that $R_0(m/n)$ is maximised when vectors display 'host patch fidelity', i.e. for each vector type r there exists some host type i_r such that $\gamma_{ri_r} = 1$ (noting that in this case the system is no longer connected).

We consider a population with $m = 2$ host types and $n = 2$ vector types, with heterogeneity only in the biting preference parameters γ_{ri}, with other parameter values as in Table 1, and with 20% of hosts being of type 1, so $(h_1, h_2) = (0.2, 0.8)$, and 50% of vectors being of each type, so $(\upsilon_1, \upsilon_2) = (0.5, 0.5)$.

We vary the biting preference parameter γ_{11} while holding constant the value of $\bar{\gamma}_{11} = \upsilon_1\gamma_{11} + \upsilon_2\gamma_{21}$, the proportion of all bites that are on hosts of type 1, and recall that $\gamma_{12} = 1 - \gamma_{11}$, $\gamma_{22} = 1 - \gamma_{21}$. In order that all parameter values be positive we require $\max\{0, (\bar{\gamma}_{11} - \upsilon_2)/\upsilon_1\} < \gamma_{11} < \min\{1, \bar{\gamma}_{11}/\upsilon_1\}$. Provided $\upsilon_1 \leq \upsilon_2$, then taking $\bar{\gamma}_{11} = \upsilon_1$ allows γ_{11} to vary over the full range $(0, 1)$, and so we set $\bar{\gamma}_{11} = \upsilon_1 = 0.5$. The case of a single vector type is recovered when $\gamma_{11} = \bar{\gamma}_{11} = 0.5$. We obtain 'host patch fidelity' when $\gamma_{11} = 0$ and when $\gamma_{11} = 1$.

From Fig. 7(a), we see that the basic reproduction number R_0 is minimised for $\gamma_{11} = 0.5$, corresponding to the model with $n = 1$ vector

type, and maximised for $\gamma_{11} = 0$ and $\gamma_{11} = 1$, corresponding to host patch fidelity. This confirms the results of [8] that vector patchiness, in addition to host patchiness, cannot decrease the value of R_0 compared to the case of host patchiness alone, and that R_0 is maximised when vectors display host patch fidelity. In contrast, we see from Fig. 7(b) that the overall endemic prevalence level $\sum_{i=1}^{m} x^*_{Hi}$ of the deterministic model is maximised for $\gamma_{11} = 0.5$ (corresponding to a single vector type) and minimised for $\gamma_{11} = 0$ and $\gamma_{11} = 1$ (host patch fidelity). From Fig. 7(c) we see that the expected persistence time of infection follows a similar pattern to R_0, being minimised in the case corresponding to a single vector type ($\gamma_{11} = 0.5$) and maximised in the case of host patch fidelity ($\gamma_{11} = 0$ or $\gamma_{11} = 1$). The endemic prevalence level of the deterministic model is once again seen to provide a rather poor guide to expected persistence times.

Note that we are not comparing to the homogeneous case here, but rather investigating the effect of host patchiness in a model already incorporating vector patchiness. For the homogeneous case $m = n = 1$ with parameter values given in Table 1 we have $U(\mathbf{0}) \approx 0.1112$, so that expected persistence time is considerably increased by the heterogeneity represented in Fig. 7(c), relative to the homogeneous case. We also see from Fig. 7(c) that $\tilde{U} = -\boldsymbol{x}^{*T}\boldsymbol{\theta}^*/2$ is not a very close approximation to $U(\mathbf{0})$ here, which is to be expected, since corresponding values of R_0 (Fig. 7(a)) are considerably greater than 1.

4. Discussion

We began, in Section 2, by studying the effect of varying parameter values upon expected persistence time of infection for the stochastic Ross–Macdonald model, starting from quasistationarity. Our results for this model largely confirm those of [5], our main aim in Section 2 having been to develop a more accurate and reliable methodology than that of [5], before going on to apply this methodology in Section 3 to investigate the effects of population heterogeneities. In [5], the quasistationary distribution was approximated using a bivariate normal distribution, which works well in approximating the central part of the distribution, but fails in the tail of the distribution relevant to extinction. The bivariate normal approximation imposes a relationship of the form (8), but with the additional constraint that the function $U(\boldsymbol{x})$ is required to be quadratic in its arguments. We assume no such restrictive form for $U(\boldsymbol{x})$, allowing considerably greater flexibility in the approximation. Consequently, a more accurate approximation in the relevant tail of the distribution is obtained. In particular, our approach yields correct asymptotic behaviour as expressed in the relationship (9), something that is not available via the normal approximation.

We found that varying any one model parameter in such a way as to increase the basic reproduction number R_0 results in a corresponding increase in expected persistence time, but that knowledge of the value of R_0 (together with host population size N) is not sufficient to fully determine the expected persistence time. This is very much as one might expect. Fig. 1 indicates how sensitive the expected persistence time is to variation in each individual parameter value. Our results differ from those of [5] in that we found the least influential parameter to be the mean host infectious period σ^{-1}, with the second least influential being the vector to host transmission probability p, whereas in the results of [5] the ordering of these two parameters is reversed. To check the ordering of parameters, we solved Eq. (5) for the expected persistence time τ directly for a small population size, with results shown in Fig. 2, confirming the pattern seen in Fig. 1 and the correctness of our ordering. However, we also saw that our numerical estimates of expected persistence time are far from accurate (although still an improvement upon those obtained from normal-based approximation). This reflects the crude nature of the asymptotic relationship (9).

For certain population models, including some infection models, it is possible to solve the Hamilton–Jacobi equation satisfied by the function corresponding to $U(\boldsymbol{x})$ in Eq. (8) analytically [19–21]. Further analysis [19,21], making use of this explicit form for $U(\boldsymbol{x})$, then leads to a relationship of the more precise form

$$\lim_{N\to\infty} \frac{\tau}{K\exp(NU(\mathbf{0}))/\sqrt{N}} = 1, \tag{28}$$

where the values of $U(\mathbf{0})$ and K depend upon model parameter values, but not upon N. Sufficient conditions for a relationship of the form (28) to hold, together with explicit formulae for $U(\mathbf{0})$ and K, are given in [21]. The relationship (28) may be expected to provide considerably more accurate estimates of τ than are available from the cruder relationship (9) — see, for instance, Fig 1 of [20]. Unfortunately, the Ross–Macdonald model and its heterogeneous population extension do not satisfy the conditions set out in [21], an explicit form for $U(\boldsymbol{x})$ is not available, and it is unclear how one might go about establishing a relationship of the form (28). We have however seen (Fig. 2 and comments in Section 2.3) that the relationship (9) does provide a reliable guide to the effects of varying parameter values upon the persistence time of infection.

In Section 3 we extended our methodology to study the effects of population heterogeneities upon persistence time. A somewhat counter-intuitive result is that the endemic prevalence level in the host population predicted by the deterministic model does not provide a good guide to expected persistence time, and that an increase in the one (as parameter values are varied) can correspond to a decrease in the other. The resolution of this is straightforward: an increase in endemic prevalence level can be accompanied by an increase in stochastic variability, with the overall effect being that extinction occurs, on average, more quickly. The absence of any clear relationship between endemic prevalence level and expected persistence time nevertheless remains somewhat surprising. We also observed, in Section 3.4, that both endemic prevalence level and expected persistence time can vary with model parameters while R_0 remains constant. The effect observed in Fig. 6(b), where increasing heterogeneity in infectious periods (with R_0 held fixed) corresponds to a decrease in disease persistence time, is in agreement with the result for a directly transmitted infection illustrated in Fig. 3 of [20].

The methodology that we have adopted for estimating persistence time, employing a WKB approximation to the quasistationary distribution, has seen a lot of interest in the theoretical physics literature (see [13] and references therein), but rather less in the mathematical biology literature, with a few recent exceptions [20,22–24]. The lack of uptake so far of this methodology amongst the epidemic modelling community may be due to the computational difficulty of implementation. For any compartmental epidemic model, it is straightforward to write down the Hamiltonian, and hence the relevant characteristic ordinary differential equations, and the equations satisfied by the equilibrium points $\boldsymbol{x}^*, \boldsymbol{\theta}^*$. For some models it is possible to solve for $\boldsymbol{x}^*, \boldsymbol{\theta}^*$ algebraically; often it is necessary to employ a numerical solver, but in general this presents no difficulties. The difficulty comes in solving the characteristic ordinary differential equations, since the relevant solution trajectory is maximally sensitive to perturbations, causing problems for numerical solvers. This problem is greatly ameliorated for models with susceptible–infectious–susceptible (SIS) structure, including the models we have considered here, because the solution trajectory is in this case not too far from being a straight line. This means, firstly, that we can approximate the trajectory by a straight line to obtain our explicit approximation $\tilde{U}$ to $U(\mathbf{0})$; and more importantly, that using a straight line as our initial guess can give good convergence of the numerical ordinary differential equation solver. Even here, an element of trial and error is required in choosing values for the scaling parameters λ and λ' described in Sections 2.2 and 3.2. Computational issues are discussed in more depth in [15].

Declaration of competing interest

The authors declare that they have no known competing financial interests or personal relationships that could have appeared to influence the work reported in this paper.

Acknowledgement

J.J.H.S. was supported by The Maxwell Institute Graduate School in Analysis and its Applications, a Centre for Doctoral Training funded by the UK Engineering and Physical Sciences Research Council (grant EP/L016508/01), the Scottish Funding Council, Heriot-Watt University and the University of Edinburgh, UK.

Appendix. Characteristic ordinary differential equations for the heterogeneous population model

For the heterogeneous population model of Section 3, with Hamiltonian given by Eq. (15), the characteristic ordinary differential Eqs. (10) are as follows.

$$\left.\begin{aligned}
\frac{dx_{Hi}}{dt} &= \sum_{r=1}^{n} x_{Vr}\alpha_{ri}\left(1-\frac{x_{Hi}}{h_i}\right)e^{\theta_{Hi}} - \sigma_i x_{Hi}e^{-\theta_{Hi}} \text{ for } i=1,2,\dots,m,\\
\frac{dx_{Vr}}{dt} &= \sum_{i=1}^{m} \frac{x_{Hi}}{h_i}\beta_{ir}(cv_r - x_{Vr})e^{\theta_{Vr}} - \delta_r x_{Vr}e^{-\theta_{Vr}} \text{ for } r=1,2,\dots,n,\\
\frac{d\theta_{Hi}}{dt} &= \sum_{r=1}^{n} x_{Vr}\frac{\alpha_{ri}}{h_i}\left(e^{\theta_{Hi}}-1\right) - \sum_{r=1}^{n}\frac{\beta_{ir}}{h_i}(cv_r - x_{Vr})\left(e^{\theta_{Vr}}-1\right)\\
&\quad -\sigma_i\left(e^{-\theta_{Hi}}-1\right) \text{ for } i=1,2,\dots,m,\\
\frac{d\theta_{Vr}}{dt} &= -\sum_{i=1}^{m}\alpha_{ri}\left(1-\frac{x_{Hi}}{h_i}\right)\left(e^{\theta_{Hi}}-1\right) + \sum_{i=1}^{m}\frac{x_{Hi}}{h_i}\beta_{ir}\left(e^{\theta_{Vr}}-1\right)\\
&\quad -\delta_r\left(e^{-\theta_{Vr}}-1\right) \text{ for } r=1,2,\dots,n.
\end{aligned}\right\} \tag{A.1}$$

References

[1] R. Ross, The Prevention of Malaria, John Murray, London, 1911.
[2] G. Macdonald, The Epidemiology and Control of Malaria, Oxford University Press, London, 1957.
[3] I. Nåsell, On the quasi-stationary distribution of the Ross malaria model, Math. Biosci. 107 (1991) 187–207.
[4] A.L. Lloyd, J. Zhang, A. Morgan Root, Stochasticity and heterogeneity in host-vector models, J. R. Soc. Interface 4 (2007) 851–863.
[5] T. Britton, A. Traoré, A stochastic vector-borne epidemic model: quasi-stationarity and extinction, Math. Biosci. 289 (2017) 89–95.
[6] J. Matthews, A. Bethel, G. Osei, An overview of malarial Anopheles mosquito survival estimates in relation to methodology, Parasites Vectors 13 (2020) 233.
[7] C. Dye, G. Hasibeder, Population dynamics of mosquito-borne disease: effects of flies which bite some people more frequently than others, Trans. R. Soc. Trop. Med. Hyg. 80 (1986) 69–77.
[8] G. Hasibeder, C. Dye, Population dynamics of mosquito-borne disease: persistence in a completely heterogeneous environment, Theor. Popul. Biol. 33 (1988) 31–53.
[9] D. Clancy, E. Tjia, Approximating time to extinction for endemic infection models, Methodol. Comput. Appl. Probab. 20 (2018) 1043–1066.
[10] M. Bartlett, The relevance of stochastic models for large-scale epidemiological phenomena, JRSS C 13 (1964) 2–8.
[11] S.N. Ethier, T.G. Kurtz, Markov Processes: Characterization and Convergence, Wiley, New York, 2005.
[12] J.N. Darroch, E. Seneta, On quasi-stationary distributions in absorbing continuous-time finite Markov chains, J. Appl. Probab. 4 (1967) 192–196.
[13] M. Assaf, B. Meerson, WKB theory of large deviations in stochastic populations, J. Phys. A 50 (2017) 263001.
[14] L.C. Evans, Partial Differential Equations, second ed., American Mathematical Society, Providence, Rhode Island, 2010.
[15] D. Clancy, J.J.H. Stewart, Computing the extinction path for epidemic models, 2023, in preparation.
[16] D.J. Wilkinson, Stochastic Modelling for Systems Biology, second ed., CRC Press, Boca Raton, Florida, 2018.
[17] R. Sundberg, Comparison of confidence procedures for type I censored exponential lifetimes, Lifetime Data Anal. 7 (2001) 393–413.
[18] A. Lajmanovich, J.A. Yorke, A deterministic model for gonorrhea in a non-homogeneous population, Math. Biosci. 28 (1976) 221—236.
[19] M. Assaf, B. Meerson, Extinction of metastable stochastic populations, Phys. Rev. E 81 (2010) 021116.
[20] D. Clancy, Precise estimates of persistence time for SIS infections in heterogeneous populations, Bull. Math. Biol. 80 (2018) 2871–2896.
[21] D. Clancy, Quasistationarity and extinction for population processes, 2023, in preparation.
[22] O. Ovaskainen, B. Meerson, Stochastic models of population extinction, Trends Ecol. Evol. 25 (2010) 643–652.
[23] G.T. Nieddu, L. Billings, J.H. Kaufman, E. Forgoston, S. Bianco, Extinction pathways and outbreak vulnerability in a stochastic Ebola model, J. R. Soc. Interface 14 (2017) 20160847.
[24] D. Clancy, Persistence time of SIS infections in heterogeneous populations and networks, J. Math. Biol. 77 (2018) 545–570.